The Electronic Properties of Cu_2CoSiS_4, Cu_2CoGeS_4, and Cu_2CoSnS_4: A DFT Approach

Omehe N. N.
Federal University, Otuoke, Bayelsa State, Nigeria
omehenn@fuotuoke.edu.ng

DOI: 10.56201/rjpst.v6.no3.2023.pg105.118

Abstract

Cu_2CoSiS_4, Cu_2CoGeS_4, and Cu_2CoSnS_4 crystallize in the stannite (I-42m) structure, and their electronic properties have been investigated by the pseudopotential method within the framework of the density functional theory (DFT). The LDA+U technique and the projector augmented wave (PAW) were employed in the computations. The results of the calculations showed these materials are metallic with pseudo band gap. The respective pseudo band gap for Cu_2CoSiS_4, Cu_2CoGeS_4, and Cu_2CoSnS_4 are 1.52 eV, 2.96 eV, and 1.2 eV. The isolated subband at the Fermi level for Cu_2CoSiS_4 are of Co-3d states, the Si-3s and Si-3p states are the dominate states in the conduction band. The top of the valence band of Cu_2CoGeS_4 is predominately of the S-3p and Ge3d states, while the bottom of the conduction is majorly of Ge-3d and Ge-4s states. For Cu_2CoSnS_4 compound, the valence band top is majorly of S-3p; and the conduction band is of Sn-5s and Co-3d.

Introduction

The group I_2-II-IV-VI_4 system of compounds have attracted a lot of attention due to their wide range of applications. Cu_2CoSiS_4, Cu_2CoGeS_4, and Cu_2CoSnS_4 are members of this group of semiconductors. The elemental constituent of this system are earth abundant and eco-friendly. They find usefulness in thermoelectricity and photo detectors (Krishnaiah et al., 2021; Zhang et al., 2017; Murali and Krupanidhi 2013; Khouja et al., 2022), Photovoltaic and photocatalytic applications (Hammami et al., 2021, Murali et al., 2014; Xie et al., 2017).

Experimentally, Gulay et al., (2004), investigated $Cu_2CoSi(Ge,Sn)S_4$ and $Cu_2CoSnSe_4$ films by X-ray powder diffraction. Their findings showed that Cu_2CoSiS_4 has the stannite structure and Lattice parameters a=0.52644 nm, c=1.0316 nm. Quintero et al., (2014), used X-ray diffraction technique to analysis samples of Cu_2CoSiS_4 crystals grown from its elemental constituents, Lattice parameters and atomic positions were reported, the respective values for a and c are 5.2693 Å and d 10.3363 Å. Quintero et al., (2014) in their study of Cu_2–II-IV-$S_4(se_4)$ magnetic semiconductors compounds, used the melt and anneal technique to synthesis samples of these compounds, and reported on structure and thermodynamic properties of the materials. Samples of Cu_2CoSnS_4 were prepared by Murali et al., (2014) via Facile So1-gel method. Their analysis showed a band gap of 1.4 eV, they also reported on the photosensitivity of the compound. Ghosh et al., (2016) prepared samples of Cu_2FeSnS_4, Cu_2FeSnS_4 and Cu_2NiSnS_4 and analysis was done using Raman spectroscopy. DFT was used to predict the band gaps of these thin films as 1.87 eV, 1.57 eV and 1.74 eV respectively. Xie et al., (2017) synthesis the films of Cu_2XSnS_4 (X=Mn, Fe,Co, Ni, Zn, and Cd) Via solvothermal technique,

and analysed by X-ray diffraction (XRD), X-ray photoelectron spectroscopy (XPS), energy dispersive spectroscopy (EDS), transmission electron microscopy (TEM), and Scanning electron microscopy (SEM). Using the facile spray deposition pyrolysis, Malder et al., (2017), prepared thin films of Cu_2CoSnS_4, and investigated the effect of substrate temperature on the properties and structure of Cu_2CoSnS_4 films. They reported on the structure, oxidation state and energy band gap. The reported range of energy band gap value is 1.42 eV to 1.79 eV. Cu_2CoSnS_4 thin films synthesized by co-electrodeposition technique grown on Molybdenum substrate were studies by Beraich et al via XRD, Raman Spectroscopy, SEM and EDS, a band gap of 1.56 eV was reported. Ghediya et al., (2019) in the work, effect of solvents on physical properties of direct-coated Cu_2CoSnS_4 films, studied the effect of film's thickness and solvent type on the optical band gap of the material. Beraich et al., (2020) synthesized thin films of Cu_2CoGeS_4 by spray method. The samples were studied via EDS and XRD, reported on sample stoichiometry and morphology, from their DFT computations, a band gap of 1.75 eV was obtained. Nanocrystals of Cu_2CoSnS_4 (CCTS) were investigated by XRD, Raman Spectroscopy, UV-VIS spectroscopy and photoluminescence study. The Nanocrystals were synthesized via solvothermal technique. The photocatalytic properties of CCTS were reported. Cu_2CoSnS_4 thin film solar cells were grown by Onah and Ekpe (2021) by chemical bath method. The samples analysis was carried out using spectrophotometer. The study renealed a refractive index of n=1.01. Effects of copper concentration on the properties of Cu_2CoSnS_4 thin film was investigated by Oubakalla et al., (2022). The Raman study showed two peaks at 290 cm and 325 cm while Uv-vis spectrophotometry showed an optical band gap value ranging from 1.48 eV to 1.68 eV.

Krishnaiah et al., (2021) prepared crystals of Cu_2CoSnS_4 on soda-lime glass substrates via spin coating technique. Analysis was done by Thermogravimetric analysis (TGA), Fourier-transform infrared spectroscopy (FTIR), X-ray diffraction and Raman studies. They reported on resistivity and photoresponsivity of the samples. The synthesis, growth and characterization of Cu_2CoSnS_4 thin films via thermal evaporation was carried out by Hammani et al., (2021). Samples of Cu_2CoSnS_4 thin films were grown on heat treated substrate and analysed by XRD, Raman spectroscopy and UV-Vis-NIR spectrophotometer. They reported on a single crystal phase, an optical absorption of 10^5 cm^{-1}, and a range of band gap value of 1.4 eV to 1.43 eV. The sol-gel spin- coating method was used by Kissani et al, (2022) to prepare thin films of Cu_2CoSnS_4, Studied by XRD, Raman spectroscopy, scanning electron microscopy (SEM), and energy dispersive analysis. They reported on the effect of annealing temperature on the properties of the thin films; and an optical band gap of 1.4 eV and an absorption coefficient of 10^4 cm^{-1}. Khouja et al., (2022), synthesized Cu_2CoSnS_4 films by spray Pyrolysis. The resulting crystal samples were subjected to XRD analysis. A stannite structure was reported for the films. Harrathi et al., (2023), deposited films of Cu_2CoSnS_4 cyrstals on glass substrate using spray Pyrolysis, and analysis was carried out via XRD, they reported on the morphology of the surface, absorption coefficient greater than 10^4 cm^{-1}, and a band gap of 1.75 eV. The effect of sulphur concentration on the structure, optical and electrical properties of Cu_2CoSnS_4 films was studied by Senguler et al., (2023). The crystals were grown on glass by sol-gel method, Raman spectroscopy, SEM and Atomic force microscopy (AFM) were used in the sample analysis. Report was made on the sample structures, that is, its different phases, its morphology, and electrical properties. A band gap range of 1.4 eV to 1.7 eV was observed.

In this work, the DFT+U method in conjunction with the Projector augmented wave (PAW) will be used to investigate the electronic properties of Cu_2CoSiS_4, Cu_2CoGeS_4, and Cu_2CoSnS_4.

Computational details

Cu_2CoSnS_4, Cu_2CoGeS_4, Cu_2CoSnS_4 compounds crystallizes in the stannite structure, belonging to the symmetry group I-42m. The group IV atoms (S in this case) is neighbor to four atoms, two group I (CU) atoms, one group II (Co) atom, and one group IV (Si, Ge, Sn) atom, located at the corners of a tetrahedron. In the crystallographic table, the groups I, II IV, and VI occupy the sites 4d, 2a, 2b, and 8i. There are two formula unit in a unit cell, making a total of 16 atoms per cell. The density functional theory plus U (DFT+U) approach in conjunction with projector augmented wave was employed in the investigation. All calculations were performed using the Abinit suite of packages (Gonze et al, 2002) Gonze et al, 2005). The inputs for this work, that is, lattice parameters and atomic positions were adopted from Gulag et al., (2004). The computed properties are the electronic band structures, total density of states (TDOS), and partial density of states (PDOS). The tolerance used on energy was 10-10 Ha/Br, cutoff kinetic energy was 15 Ha and K-point of 256. Table I shows the input parameter employed in the computation. The valence states included in the calculations are Cu:3s,3d,4s; Sn: 4d,5s,5p; Ge:3d,4s,4p; S:3s,3s,3p; Si:3s,3p; Co:3s,3p,3d,4s.

Table 1: Lattice parameter used in the computations and adopted from Gulay et al., (2004)

	Lattice parameter (Å)
Cu_2CoSiS_4	a=5.2644 c=10.316
$CuCoGeS_4$	5.2957 10.4709
Cu_2CoSnS_4	a=5.3956 10.789

Results presentation and discussion

The electronic band structure of Cu_2CoSnS_4, Cu_2CoGeS_4, and Cu_2CoSnS_4 are presented in figures 1a to 1c respectively. The plot is energy (eV) against the high symmetry points in the first brillouin zone, and the direction of plot is along Γ-X-M-P-Γ-M. Figure 1a shows the band structure of Cu_2CoSiS_4, and it shows a direct pseudo band gap of 1.52 eV. This is so because the states proceeding the Fermi level (Fermi level indicated by dashed line) are of the conduction band. The subband about the Fermi level are isolated from both the conduction and valence band, that is, this subband is sandwich by the pseudo energy band gap and the valence intra band gap of 1.0 eV, and this subband has a dispersion width of about 0.7 eV. Another feature of the band structure is the flatness of the band at the Fermi level. This indicate that there are several transition points in the band structure. The high symmetry points X and M are notable degeneracy points. At the Γ-point, band splitting is observed at the Fermi level. Figure 1b displays the electronic band structure of Cu_2CoGeS_4, as in the case of Cu_2CoSiS_4, Cu_2CoGeS_4 show metallic behavior with an indirect pseudo band gap of 2.96 eV. The subband at the Fermi level has an energy width of about 3.8 eV, which is 3.1 eV greater than that of Cu_2CoSiS_4. The dispersion of the valence top bands is small, giving rise to multiple important critical points in the bands structure. The maximum valence band occurs at the M point of high symmetry while the conduction band minimum occurred at the Γ point of high symmetry. The experimentally reported band gap value for Cu_2CoGeS_4 is 1.75 eV (Beraich et al, 2021). The band structure of Cu_2CoSnS_4 is shown in Figure 1c, it shows the material to be a metal with a

Pseudo band gap value of 1.2 eV. There is a single conduction band just proceeding the Fermi level giving the material its metallic behavior. The pseudo band gap is indirect. Again, X and M high symmetry point are notable degeneracy points in the band-structure and this has implication in thermoelectric applications. The experimentally observed band gap has been report to be about 1.4 eV to 1.79 eV (Ghost et al, 2016; malder et al, 2027; Beraich et al, 2019; senguler et al., 2023).

(1a) (1b)

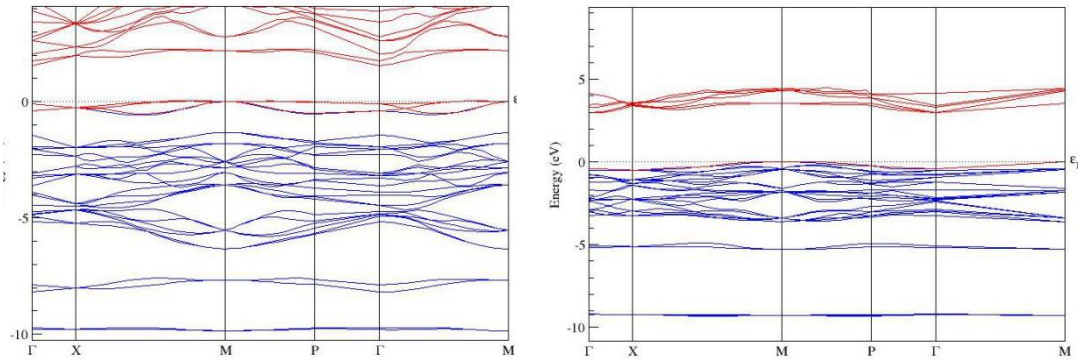

(1c)

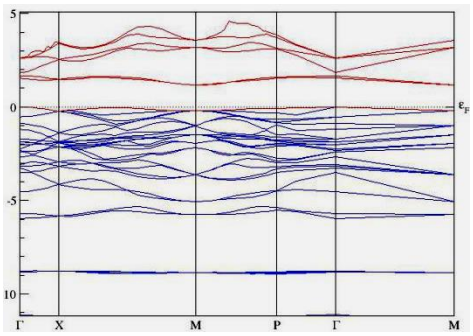

Figure 1: Electronic band structure of (1a) Cu_2CoSiS_4 (1b) Cu_2CoGeS_4 and (1c) Cu_2CoSnS_4.

The total density of states (TDOS) for Cu_2CoSiS_4, Cu_2CoGeS_4, and Cu_2CoSnS_4, are presented in Figure 2a to 2c respectively. The features of the graphs present the various valence orbitals or states included in the projector augmented wave (PAW) pseudopotentials used in the band structure calculations. For Cu_2CoSiS_4, its TDOS is displayed in Figure 2a. The energy width of the various subbands are well captured, the energy band gap is also seen near the Fermi level. The Fermi level is at the 0.2 Ha mark. The features or peak from -3.3 Ha to 0.2 Ha represents subbands with narrow dispersion. The peaks from 0 to 0.2 Ha represents the states at the valence band maximum (VBM), while the states from about 0.25 Ha to 0.4 Ha are of the conduction band. The TDOS for Cu_2CoGeS_4 is displayed in figure 2b, it shows the contributions of all the valence state of the respective elemental atoms in the compounds formula. All features in the electronic band structure are captured in the TDOS. The Fermi level is at the 0.1 Ha mark. The features from -0.1 Ha to 0.1 Ha represents the states at the VBM while that from 0.2 Ha and beyond represents that of the conduction band. The features with sharp peaks represents subbands with very narrow dispersions. For Cu_2CoSnS_4, its TDOS is presented in Figure 2c. Again, the features of the band structure are well represented in the

TDOS plot. The energy width of the various subbands are also captured. The Fermi level is at 0.15 Ha.

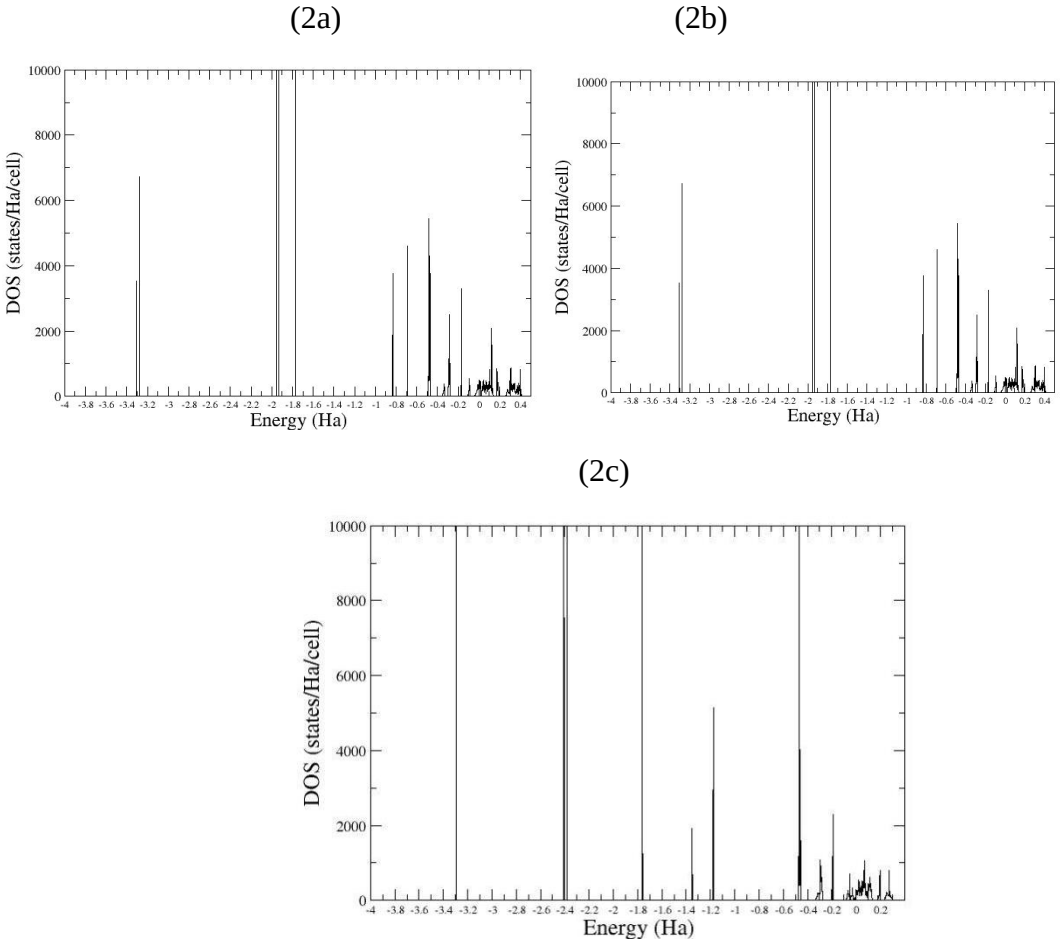

Figure 2: The TDOS for (2a) Cu_2CoSiS_4 (2b) Cu_2CoGeS_4 and (2c) Cu_2CoSnS_4.

The partial density of states (PDOS) of the various states contribution for Cu_2CoSiS_4, are described in Figures 3 to 6. The orbital contributions from the Cu atom is presented in Figure 3. The states contribution describe here are Cu-3s, 3p, 3d, and 4s states. The Cu-3s state contribution to the TDOS is represented by the feature at -3.3 Ha, the black lines in Figure 3 represents plots for Cu-3s and Cu-4s. The red lines represent that for Cu-3p and the green line for Cu-3d. The narrow peak at -1-8 Ha represents Cu-3p contribution. The Cu-3d states are represented by the feature in green at -0.5 Ha, 0.3 Ha and 0.0 Ha to 0.1 Ha. There is a negligible presence of Cu—3d in the conduction band. Most of the valence and conduction band are of the Cu-4s state. So, for Cu, much of what it contribution to VBM and CBM is the Cu-4s, and these contributions are quite small.

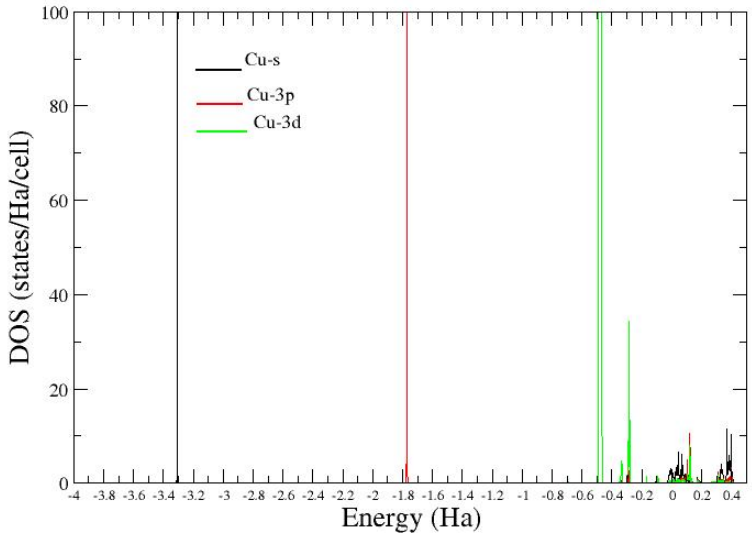

Figure 3: The PDOS of Cu orbitals in Cu_2CoSiS_4

The PDOS for Co in Cu_2CoSiS_4, is shown in Figure 4. The black line represents the Co-3s and Co-4s states, the red is for Co-3p states, and the green for Co-3d states. The feature at -3.29 Ha represents contribution from Co-3s. The peak at -1.95 Ha is the contribution from Co-3p states while the green line features indicates the contributions from Co-3d states.Co-3d states are the dominant specie in the VBM. Co-4s state dominates the conduction band minimum. Though there is an overlaps of all three states in the conduction band. So for Co, its major contribution in the VBM is the Co-3d states. Most of the isolated subband at the Fermi level in the band structure of Cu_2CoSiS_4, are of Co-3d states as indicated in Figures 4.

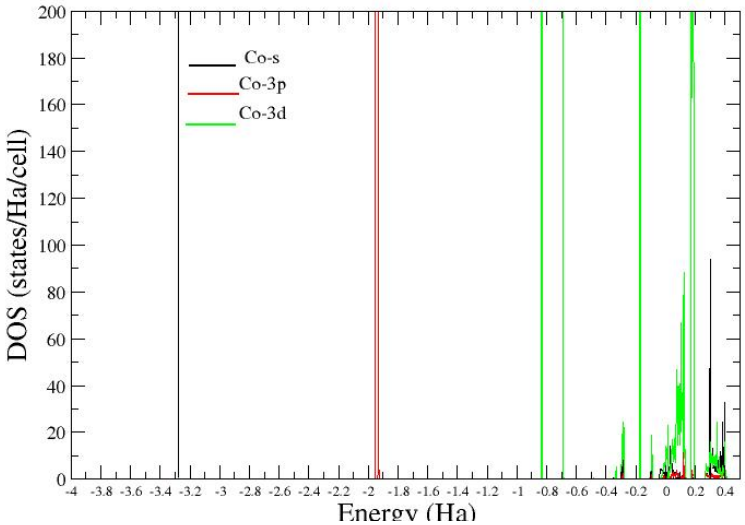

Figure 4: The PDOS of Co orbitals in Cu_2CoSiS_4.

The black and red lines in Figure 5 represent features belonging to the Si-3s and Si-3p states respectively. The peaks at -3.5 Ha, about -0.1 Ha are contributions from Si-3s orbitals. The Si-

3p contributions dominates the VBM, while the conduction band shows an overlaps of both Si-3s and Si-3p states.

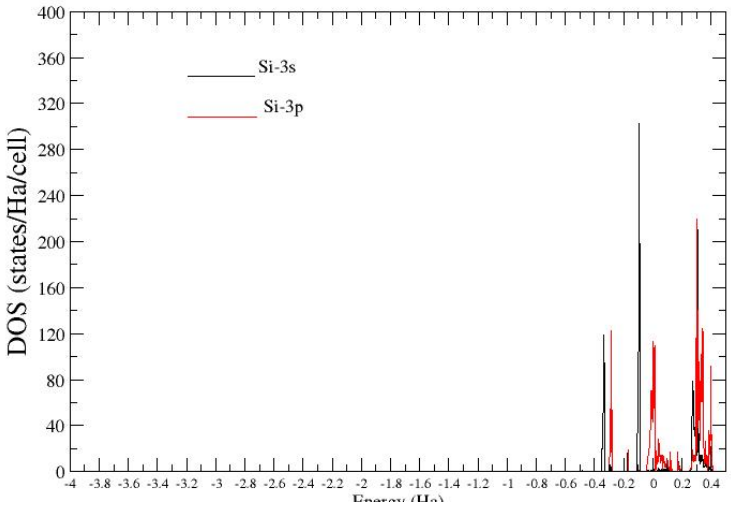

Figure 5: The PDOS of Si orbitals in Cu_2CoSiS_4.

Figure 6 show the S-3s and S-3p states contributions to the TDOS of Cu_2CoSiS_4, As usual, the black line represents contribution from S-3s and the red line for S-3p states. It can be seen that the features about -3.3 Ha and -3.5 Ha belong to contributions from S-3s while much of the valence band is dominated by S-3p states. The conduction band shows an overlap of both the S-3s and S-3p states. So for Cu_2CoSiS_4, VBM is predominantly of the Co-3d and S-3p states, but the S-3p is the dominant states in the VBM while for the conduction band, the Si-3s and Si-3p are the major states.

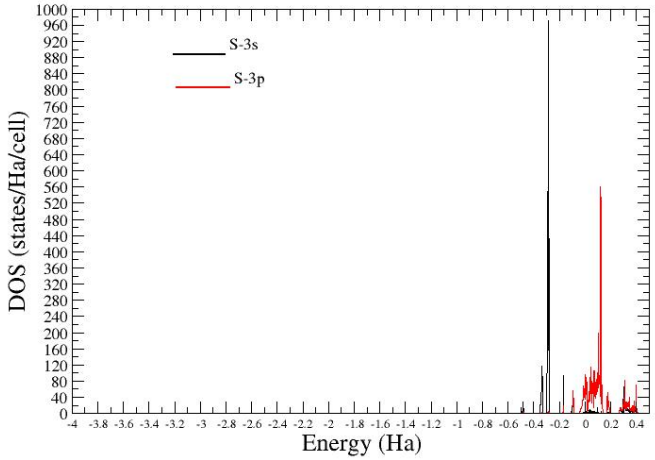

Figure 6: The PDOS of S orbitals in Cu_2CoSiS_4

The PDOS for the elemental orbitals of Cu_2CoGeS_4, are presented in figures 7 to 11. The orbital contributions from the Cu atoms is shown in figure 7. The features for Cu-3s and Cu-4s are depicted by black lines, Cu-3p by red line, and Cu-3d by green line. The Fermi energy is at 0.1 Ha. the feature or peaks at -3.3 Ha, -1.8 Ha represents states contributions from Cu-3s and Cu-

3p respectively. The Cu-3d state contribution can be seen at -0.7 Ha, -0.3 Ha and at the VBM. The rare of theVBM is dominantly Cu-4s.

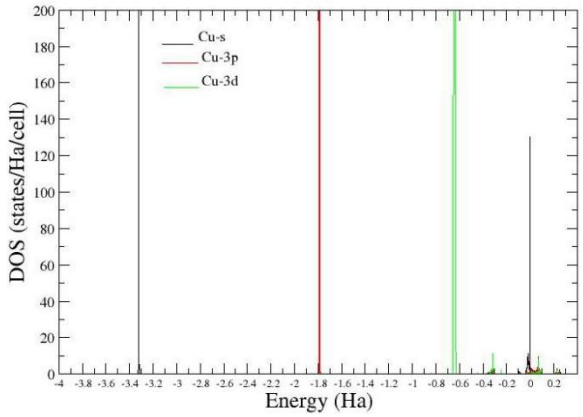

Figure 7: The PDOS of Cu orbitals in Cu_2CoGeS_4

Co atom contribution to TDOS is displayed in Figure 8. The features at -3.0 Ha and the twin peaks at -1.70 Ha and -1.05 Ha are of Co-3s and Co-3p respectively. Co-3d dominates the valence band maximum.

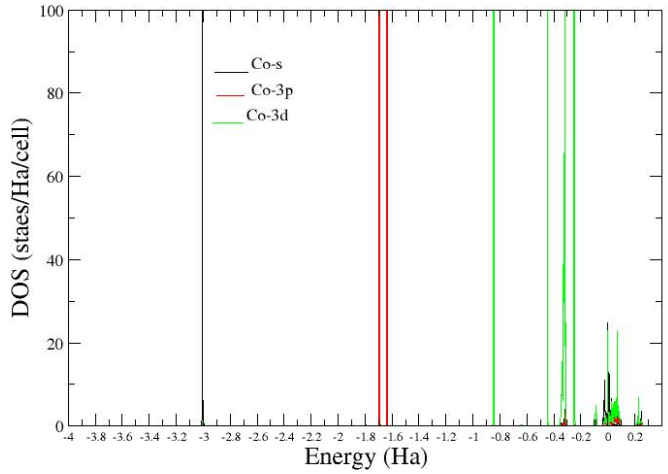

Figure 8: The PDOS of Co orbitals in Cu_2CoGeS_4

For Ge, its contributions to TDOS is presented in figure 9. The black, green, and red lines represent features of the state densities associated with Ge-4s, Ge-3d, and Ge -3p respectively. As seen from Figure 9, Ge-3d states dominates the top of the valence bands, while the conduction band is predominantly Ge-3d and Ge -4s. The Ge-4p contribution is very small, and can be seen at the VBM.

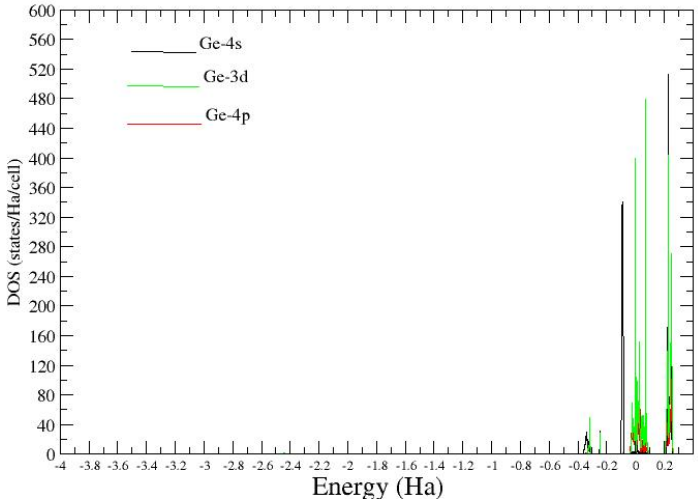

Figure 9: The PDOS of Ge orbitals in Cu_2CoGeS_4

Figure 10 shows PDOS for the S atom. The features between -0.2 Ha and -0.4 Ha belong to S-3s contributions while the top of the valence band is also predominantly S-3p states. For Cu_2CoGeS_4 TDOS, the top of the valence band is predominantly of the S-3p and Ge-3d states while the bottom of the conduction band is majorly of Ge-4d and Ge -4s states.

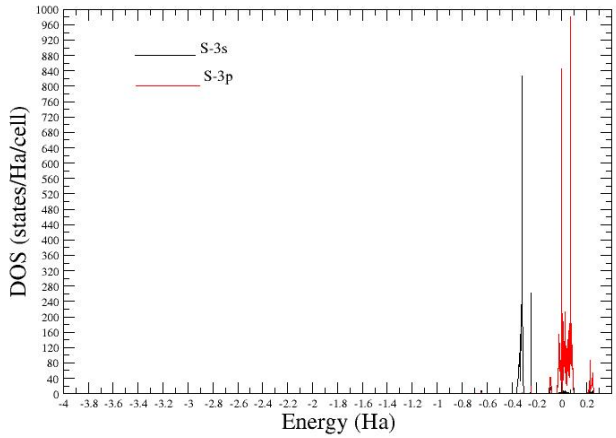

Figure 10: The PDOS of S orbitals in Cu_2CoGeS_4

The orbital decomposition of Cu_2CoSnS_4, are presented in Figures 11 to 14. For Cu atoms, the represented states are Cu-3s, Cu-3p, Cu-3d and Cu-4s. there are displayed in Figure 11. Cu-3s and Cu-3p contribution to the density of states are represented by the features at -3.3 Ha, and -1.8 Ha respectively, while Cu-3d is represented by the peaks at -0.3 Ha and -0.1 Ha. Also, a small contribution from Cu-3d is at the top of the valence band. Cu-4s is also a small contribution at the top of the valence.

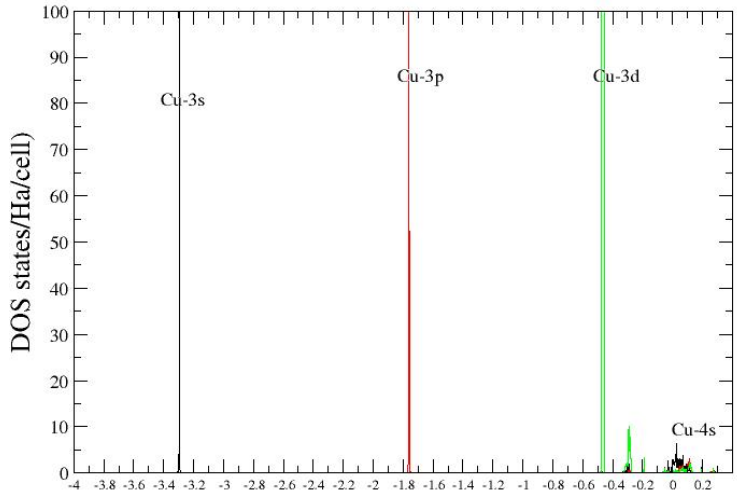

Figure 11: The PDOS of Cu orbitals in Cu_2CoSnS_4

For Co, its contribution to TDOS is presented in Figure 12. The red line features represent contributions from Co-3p at -2.4 Ha. The localized peaks at -1.4 Ha and -1.2 Ha represents contributions from Co-3d states. The Co-4s state is at the rear of the subband at the VBM at about 0.1 Ha. the Co-3d states contribution dominates the top of the valence band and the conduction band.

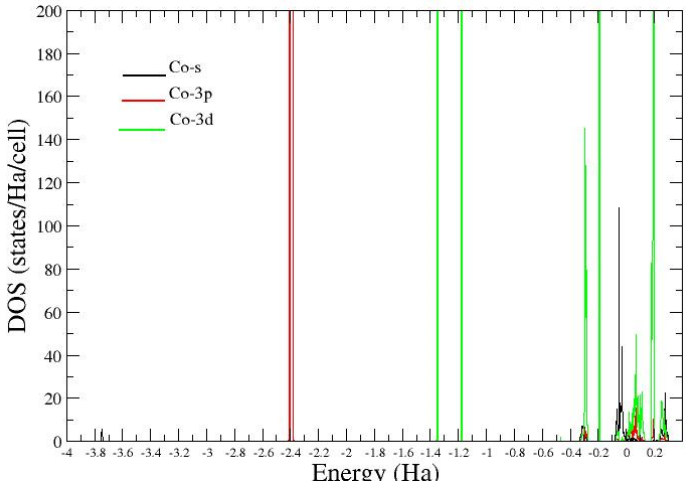

Figure 12: The PDOS of Co orbitals in Cu_2CoSnS_4

The Sn atom contribution is displayed in Figure 13. The small contributions from Sn-4d it seen at -1.9 Ha and -0.1 Ha. It also has negligible contributions between the zero mark and the Fermi level. The Sn-5s state contribution is between 0 Ha and 0.1 Ha. it is the dominate state in the conduction band. Sn-5p orbitals are the dominant state between 0 and the Fermi energy Co-15 Ha) are the dominant state between 0 and the Fermi energy (0.15 Ha).

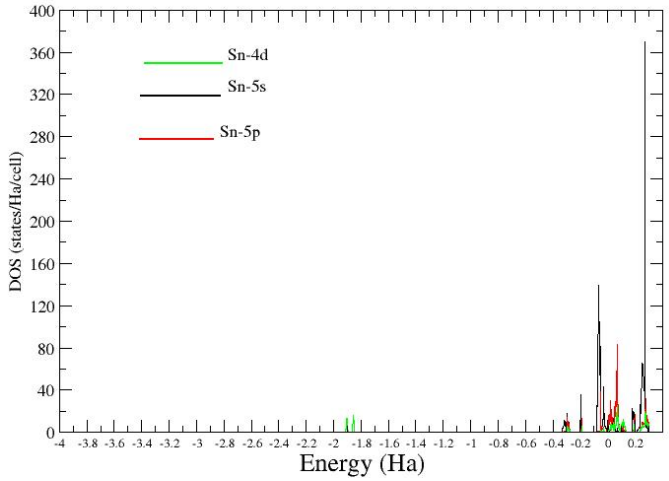

Figure 13: The PDOS of Sn orbitals in Cu_2CoSnS_4

Figures 14 shows the PDOS of S atom. S-3s states are represented by the peaks within the energy range from -0.4 Ha to -0.2 Ha, while S-3p states contribution dominates the topmost subband of the valence band and the conduction band. So for Cu_2CoSnS_4, the top of the valence band is majorly of S-3p while conduction band is predominantly of Sn -5s and Co-3d States.

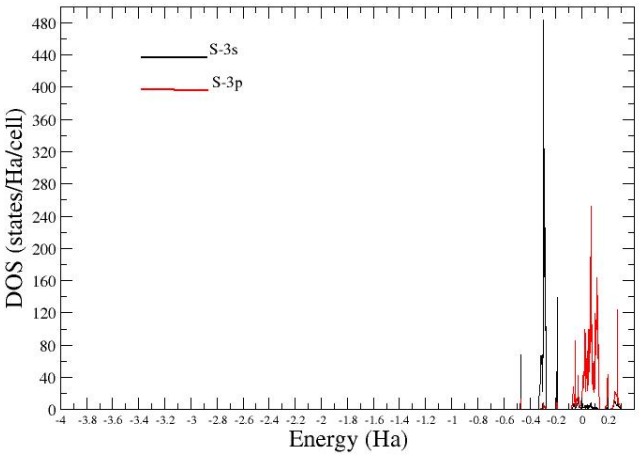

Figure 14: The PDOS of S orbitals in Cu_2CoSnS_4

Conclusion

The materials under investigation have elemental compositions that are earth abundant and non toxic to the environment. These materials also have technological applications especially in Photonics. They have been studied via DFT, using the pseudopotential method. The calculations showed these materials to have pseudo band gaps and have various degrees of metallicity.

References

Anima Ghosh, Amrita Biawas, Rajalingam Thangavel, and Udayabhanu G. (2016), Photo-electrochemical properties and electronic band structure of kesterite copper chalcogenide Cu_2-II-SnS_4 (II=Fe, Co, Ni) thin films. Royal Society of Chemistry (RSC) Advances. Issue 98, 96025-96034.

Banavoth murali B and Krupanidti S. B. (2013), Facile Synthesis of Cu2CoSnS4 nanopartiicles Exhibiting red-edge effect: Application in hybrid photonic devices, J. Appl. 114, 144312, Https://doi.org/10.1063/1.4825070.

Baraich M., Taibig M, Guenbour A., Zarrouk A., Boudaila M., Bellaouchou A., Tabyaoui M., Sekkat Z., Fahoume M. (2019), Synthesis and Characterization of Cu2CoSnS4 Ethin Film Via Electro deposition technique for solar cells, J. Mater. Sci: Mater. Elect, Vol. 30, (13).

Beraich M., Shaili H., Hafidi Z., Abderrahim el Hat, Taibi M., Bentiss F., Quenbour A., Mansouri S., Mzred A., Fahoume A. M.. (2020), Structural electronic and optical properties of a tetragonal –stannite Cu_2CoGeS_4 Etin film synthesized by a low cost spray method. Experimental and theoretical study, Ceramics Int. Vol 46, iss. 14, 23127-23133, Doi:10.10/6/j.ceramint.2020.06.090.

Ghediya P. R, Joshi K. K., Kasela D. A., Chaudhuri T. K., and Kandoliya M., (2019), Effect of solvents on Physical properties of Direct–coated Cu_2CoSnS_4 Films, Mater. Res. Express 6, 106419, DOI: 10.1088/2052-1591/abzae5.

Gonze X., Beuken J.-M., Caracas R., Detraux F., Fuchs M., Rignanese G.-M., Sindic L., Verstraete M., Zerah G., Jollet F., Torrent M., Roy A., Mikami M., Ghosez Ph., Raty J.-Y., and Allan D.C., (2002) First-principles computation of material properties : the Abinit software project, Computational Materials Science 25, 478-492.

Gonze X., Rignanese G.-M., Verstraete M., Beuken J.-M., Pouillon Y., Caracas R., Jollet F., Torrent M., Zerah G., Mikami M., Ghosez Ph., Veithen M., Raty J.-Y., Olevano V., Bruneval F., Reining L., Godby R., Onida G., Hamann D. R., and Allan D. C., (2005) A brief Introduction to the Abinit software package. Z. Kristallogr. 220, 558-562.

Guan H., Ma X.,, Zhao J. (2020), Synthesis and Photocatalytic Properties of Cu_2CoSnS_4 Nanocrystals with stannite and Wurtzite structure, Micro and Nano Letters: 15(4).

Gulay L. D. , Nazarchuk O.P. ,Olekseyuk E. D. (2004), Cystal structures of the compounds Cu_2Cosi (Ge,Sn)S_4 Cu_2CosGe (S_n)S_4, J. Allogs Compd. 377(1):306-311.

Hamdaoui J. E., Kamal L., Mazkad D., Beraich M., Fatimy A. E, Courel M., Perez L. M., Diaz P., Laroze D., Feddi E., (2023), First principles study on electronic and optical properties of Cu_2CoGeS_4 for photovoltaic conversion and photocatalytic opplications, Mater. Res. Bull. 164, 112235.

Hammami H., Marzougui M., Oueslati H., Rabeh M. B., Kanzari M., (2021), Synthesis, Growth and characterization of Cu_2CoSnS_4 Thin films via thermal Evaporation

Method, optik, Vol. 227, 166054.

Harrathi F., Aubry E., Dridi S., Briois P., Bitri N. (2023), Effect of the substrate temperature on the synthesis of the Cu_2CoS_4 films by spray pyrolysis for solar cells devices, J. Mater. Sci. Mater. Elect., 34(4), DOI:10.1007/5/0854-022-09720-6.

Khouja O. E., Assahsahi E, Nouneh K., Touhami M. E, Secu M., Talbi A., Khaaissa Y., Matei E., Stancu V., Galatanu A., Galca A. C. (2022), Structural and transport properties of Cu_2CoSnS_4 films prepared by spray pyrolysis, Caremics Int., Vol. 48, Issue 21 32418-32426.

Kissani A. E., Ehaj D. A., Drissi S., Abali A., Agdad A., Dads H. A., Nkhaili I., Mansouru A. E, Chaib H., Assali K. E., Outzourhit A. (2022), Structural, optical and electrical properties of Cu2CoSnS4 ethin film solar cells prepared by facile Sol-gel route, Thin Solid Films, Vol. 758, 139430.

Krishnaiah M., Jeong Y. J., Mistra R. K., Kim M. J., Song J., Jin S. H. (2021), Temperature–Time profile effects on evolution of physical and electronic properties in visible light Cu_2CoSnS_4 photo detectors, Mater. Sci Semiconductor Processing, Vol.121, 105443, https:// doi.org/10.1016/j.mssp.2020.105443.

Malder P., Gaikwad M., Mane A., Nakam S. S., Desai S. P., Giri S. D., Sarkar A., Mohokar A., (2017), Fabrication of Cu_2CoSnS_4 thin films by a facile spray pyrolysis for photovoltaic applications, Solar Energy, Vol. 158, 89-99, https://doi.org110.1016/j.solener.2017.09.036.

Murali B., Madhuri M., and krupanidhi S. B. (2014), Solution processed Cu_2CoSnS_4 Thin Films for Photovoltaic Applications, Cryst Growth Des. 14, 8, 3685-3691, https://doi .org/10.1021/cg500622f.

Onah D. U. and Ekpe J. E. (2021), Optical Properties of Kesterite $Cu_2CoS_nS_4$ thin Film solar cells, Adv. Appl. Sci. Res. 12, 9:41.

Oubakalla M., Beraich M., Taibi M., Maydoubi H., Guenbour A., Bellaoucho A., Addou M., Bentiss F., Zarrouk A., Fahoume M. (2022), Efeect of copper concentration on the properties of Cu_2CoSnS_4 thin films codeposited on the FTO substrate, J. Mater. Sci: Mater. Elect., 33(15):1-10, DOI: 10.1007/s/0854-022-08162-4 33,12017-2025.

Quinteo M., Moreno E, Alvares S., Marquina J., Rincon C., Quintero E, Grima P., Heano J-A., Macias M. A., (2014) Lattice parameter values and phase transitions for the Cu_2-II-IV $S_4(Se_4)$ (II=Mn, Fe, Co; IV= Si, Ge, Sn) magnetic semiconductor compounds, Rev. LatinAM. Metal. Mat. 34(1) 28-38.

Quintero M., Marquina J., Quintero E., Moreno E., Aivarez S., C Rincon, Grima P., Bocaranda P., Rivero D., Henao J. A., Macias M. A.(2014), X-ray diffraction analysis of stannite, Wurtz-stannite and Pseudo-Cubic quaternary compounds by Rietveld method, Rev. Mex. Fisica 60, 168-175.

Senguler G. Y., Narin E. K., Lisesirdin S. B., Serin T. (2022), Effect of sulfur concentration

on structural, optical and electrical properties of Cu_2CoSnS_4 Absorber film for photovoltaic devices, Physica B. Cond. Mat., Vol. 648, 414424.

Xie Y., Zhang C., Yang G., Yang J., Zhou X., and Ma J. (2017), Highly crystalline stannite-phase Cu_2XSnS_4 (X=Mn,Fe, Co, Ni Zn, and Cd) Nanoflower counter electrode for ZnO-Based dye–Senitised solar cell, J. Alloys Compd, Vol. 695, 938-946.

Zhang D., Yang J., Jiang Q., Zhou Z., Li X., Xin J., Basity A., Ren Y, He X. (2017), Multi-Cations Compound Cu_2CoSnS_4: DFT Calculating, band engineering and thermoelectric performance regulation, Nano Energy c, 36,156-165, DOI: 10.1016/j.Nanoen.2017.04.027.